Climate modelling and deep-time climate change

Rodrigo Caballero and Peter Lynch

Meteorology and Climate Centre, School of Mathematical Sciences
University College Dublin
Ireland

Abstract

Detailed and reliable understanding of past climate change is a key ingredient in unraveling how climate has influenced life on Earth and will continue to do so in the future. Paleoclimatology and climate modelling have both make rapid strides over the past decades, and there has been fruitful two-way interaction between the two fields. The application of climate models to paleoclimates has proved useful both in interpreting paleoclimate proxy data, and in testing the robustness and generality of climate models. Here, we give an overview of the current state of climate modelling, and review recent progress in understanding deep-time climate change, with emphasis on problems where climate models have played a salient role. By suitably adjusting the concentration of atmospheric greenhouse gases, climate models can be made to replicate many key climatic transitions in Earth's history. However, important discrepancies remain between modelled climates and proxy reconstructions, particularly on the warm end of the spectrum.

1 Introduction

Climate science deals with reconstructing and explaining the long-term mean and variability of physical conditions in Earth's envelope. A striking feature emerging from such analysis is the vast range of timescales on which there is significant variability. Part of this variability, including the diurnal and annual cycles, is periodic and predictable, but mostly it is random and unpredictable. We know from direct experience that the weather changes from hour to hour, from day to day, and from year to year. Analysis of long-term instrumental records and of paleoclimatological proxy data shows that the same is true on longer timescales: conditions change randomly from century to century, millennium to millennium, and from aeon to aeon. Figure 1 shows a composite spectrum of surface temperature and temperature proxies spanning timescales from a few days up to about 1 million years (Huybers and Curry, 2006). There are sharp peaks at the annual frequency and subannual harmonics, as expected. There are also some more poorly-defined peaks at the 41 kyr and 100 kyr orbital variability frequencies (see Wunsch, 2003, 2004, for a discussion of the statistical significance of these peaks). But most of the spectrum in fact shows very little structure, and is best approximated by straight lines of constant slope. Thus, at least on timescales up to around 1 million years, climate variability is mostly red noise—fully stochastic, unpredictable variability skewed towards low frequencies.

Time series whose spectra are red up to the lowest frequencies, such as those shown in Figure 1, are said to possess "long memory" or "long-range correlation" (Beran, 1994). A feature of long-memory processes is that any finite-length time series segment will typically show a trend, because the segment can be thought of as being "embedded" in a longer-term fluctuation. Figures 2 and 3 show temperature reconstructions over the Cenozoic (up to 65 million years ago (Ma) Zachos et al., 2001) and the Phanerozoic (up to 545 Ma Royer et al., 2004). Interestingly, both these time series show clear trends (for the Phanerozoic time series in Figure 3, this is only the case if the oxygen isotope data is appropriately corrected for pH effects; see (Royer et al., 2004)). Though this trend by itself is not enough to infer long memory, the important implication is that the climate system appears never to have been in steady state, even over time spans comparable to the age of the Earth. Life has co-evolved with climate over this time, and much remains to be understood about the way in which life and climate have mutually conditioned each other's evolution. This chapter will focus on climatic aspects, providing a backdrop for the more biologically oriented chapters in the rest of the book.

Mitchell (1976) and Kutzbach (1976) provide classic accounts of the mechanisms underlying long-term climate variability. The climate system contains two fluid components, the atmosphere and ocean, which are strongly heated in the tropics and more weakly heated in the high latitudes. This heating gradient triggers internal instabilities leading to ceaseless, chaotic motion in the ocean-atmosphere system with timescales from days to a few thousand years and spatial scales from hundreds to many thousands of kilometers (the fact that heating is stronger near the surface than aloft also triggers convective motions in the atmosphere with much shorter space and time scales). The atmosphere and ocean also interact with non-fluid components having much longer timescales. The build-up of large continental ice sheets requires on the order of 10^5 years. The long-term carbon cycle, which controls atmospheric CO_2 concentrations and thus the greenhouse effect and surface temperature, involves the slow weathering of silicate rocks (Walker et al., 1981) which sets a timescale on the order of 10^5 years for the drawdown of atmospheric CO_2. Tectonic processes, including the creation of large mountain ranges, the opening/closing of ocean seaways and the establishment of major igneous provinces, have timescales of 10^6–10^7 years. The formation and breakup of supercontinents—loosely speaking, the Wilson cycle (Wilson, 1966)—has timescales of 500 million years. At the very longest timescales, the Sun's luminosity has been steadily increasing, by perhaps 40% over geologic time. The "faint young sun" paradox—the problem of reconciling evidence for liquid water early in Earth's history with the low insolation then prevalent, first pointed out by Sagan and Mullen (1972)—has yet to be fully resolved. Finally, as noted above, the appearance and evolution of life on Earth has also had a major impact on climate, whose details have been only partially unravelled.

By comparison with Earth's previous history, the past 10,000 years (the Holocene) have been relatively quiescent, with no major swings in ice volume or sea level and relatively mild changes in global and regional temperatures. This is also the period in which agriculture and settled human society first arose. Human population and its economic activities have now reached a scale such that they may strongly impact climate at the regional and global scales. Since human society has evolved and is adapted to a particular set of climate conditions, any change is likely to result in widespread disruption and hardship. Perhaps the most alarming possibility is of a major melting of the Greenland and/or Antarctic ice sheets: total collapse of the Greenland ice sheet alone would cause sea level rise of around 7 m (Solomon et al., 2007), potentially submerging many of the world's most populous cities and driving hundreds of millions of people into destitution.

The problem of understanding the climate system and predicting its evolution in the near future has gained much prominence in scientific and public debate. The study of paleoclimates helps answer such questions as "how much?" and "how fast?" climate can change. It also serves as a testbed for theories of climate. Quantitative assessment of future climate change relies very heavily on global climate models, which contain a detailed description of the physics governing climate. Application of climate models to paleoclimates helps solve some of the puzzles posed by paleoclimates, and provides a particularly stringent test of model robustness and reliability. In the following sections, we provide a brief review of climate modelling (Section 2) and of long-term climate change (Section 3). We emphasize time periods where the interplay of models and paleoclimate proxy data has been particularly illuminating; these fall mostly (but not entirely) in the Cenozoic, where proxy data is most abundant.

2 Climate modelling

2.1 The physical basis of climate modelling

The Earth's climate is governed by fundamental and well-understood principles of physics. In weather prediction and climate models, these principles are expressed as mathematical equations which are then solved by numerical means. An excellent introduction to climate modelling is provided by (Washington and Parkinson, 2005). For an account of the evolution of numerical weather prediction models, see (Lynch, 2006).

The motions of the atmosphere and oceans evolve according to the laws of dynamics first established by Newton in the seventeenth century. These laws relate changes in the motion to the forces applied to the system: if we can identify and specify the forces, we can use the laws of motion to deduce how the system will evolve. Thus, the dynamics can be described in precise terms. However,

dynamics alone is insufficient. We also need to consider the effects of heating and cooling. These effects are described by the laws of thermodynamics and electromagnetic radiation, which were brought to light in the nineteenth century. The climate is driven by solar energy. Because of the spherical shape of the Earth, and the configuration of its orbit around the Sun, the amount of incoming solar energy is highly variable, depending strongly on the time of day, the season and the latitude. The climate system can be viewed as an enormous thermodynamic engine, with the atmosphere and oceans playing the role of the working fluid, transporting heat from source to sink regions and performing work in the process.

In addition to dynamics and thermodynamics, there is the principle of conservation of mass, which provides a quantitative relationship called the continuity equation. The physical variables are linked through a relationship known as the equation of state. Finally, the physical principles of how matter and radiation interact, and how water changes between the solid, liquid and gaseous phases, complete the picture. We can specify the state of the atmosphere-ocean system at a particular time by providing the values of the physical variables everywhere throughout the system. Thus, if we give the pressure, temperature, density and (for the ocean) salinity, and the velocity in each direction and at every point, the configuration of the system is determined. Such data are called the initial conditions. Given these conditions, the physical principles may now be used to deduce the future evolution of the system.

Each physical law has a precise mathematical expression, and the assemblage of laws provides us with a closed set of equations. Mathematicians describe these as nonlinear partial differential equations. They cannot be solved by analytical means; the solution in each case must be calculated by numerical approximations. The complete system of equations was first assembled around 1900, by scientists interested in forecasting weather by rational means. However, fifty years had to pass before this goal of numerical weather prediction began to become a reality.

In 1950 a drastically simplified mathematical model of the atmosphere was used to simulate the evolution of the weather over a one day period (Charney, Fjørtoft and von Neumann, 1950). A few years later, Norman Phillips carried out the first long-range simulation of the general circulation of the atmosphere. He used a two-level model with simplified equations and geometry, and with rudimentary physics. The computation used a spatial grid of 16x17 points, and the simulation was for a period of about one month. Idealized initial conditions were used and, during the simulated month, a state developed having some of the key features of the observed atmosphere. Starting from a zonal (westerly) flow with small random perturbations, a wave disturbance with wavelength of 6000 km developed. It had the characteristic westward tilt with height found in baroclinic waves, the large-scale unstable waves found in the mid-latitude atmosphere, and the disturbance moved eastward at about 20 m s^{-1}, which is comparable to observed atmospheric

waves. Phillips examined the energy exchanges of the developing wave and found good qualitative agreement with observations of wave systems in the atmosphere. He also examined the flow averaged around parallels of latitude, the mean meridional flow, and found circulations corresponding to the three atmospheric cells.

Phillips completed his experiment in 1955 and communicated the results to John von Neumann, who immediately recognized their significance and arranged a conference in Princeton in October 1955, "Application of Numerical Integration Techniques to the Problem of the General Circulation". For a retrospective review, see Lewis (1998). Following this conference, Phillips entered the research for the first Napier Shaw Memorial Prize. On 20 June 1956, the adjudicators recommended that the prize be given to Norman Phillips for his essay 'The general circulation of the atmosphere: a numerical experiment,' which had been published in the Quarterly Journal of the Royal Meteorological Society in (Phillips, 1956).

Phillips' work had a galvanizing effect on the meteorological community. Within ten years, there were several major research groups modelling the general circulation of the atmosphere, some of the leading ones being at the Geophysical Fluid Dynamics Laboratory in Princeton, New Jersey, the National Center for Atmospheric Research in Boulder, Colorado, the UK Met Office's Hadley Centre in Exeter and the Max Planck Institute for Climate Research in Hamburg, Germany.

2.2 Current global models

Following the seminal work of Phillips, the development of general circulation models (GCMs) advanced rapidly, hand-in-hand with increasing computer power. Standard current-generation GCMs include a detailed description of the dynamics and physics of both the atmosphere and ocean (these are referred to as "coupled" GCMs), and also incorporate sophisticated treatment of the hydrological cycle over land, and of the formation and dynamics of sea ice. For paleoclimate applications, a standard GCM can be coupled to a dynamic ice sheet model. Ice sheets evolve over timescales of 10^4 –10^5 years, far in excess of what is feasible for a continuous GCM simulation given current computer capabilities, so in this case the coupling is performed asynchronously, i.e. in a sequence of quasi-equilibrium steps. Much effort is being devoted at present to incorporating aspects of the carbon cycle, including interaction with land and ocean biota; to more refined atmospheric chemistry and aerosol schemes; and to incorporation of oxygen isotope fractionation.

As an example of a current climate model, we consider HadCM3, developed at the Hadley Centre. Many earlier coupled models needed a flux adjustment (additional artificial heat and moisture fluxes at the ocean surface) to produce good simulations. The higher ocean resolution of HadCM3 was a major factor in removing this requirement. To test its stability, HadCM3 has been run for over

1000 years simulated time and shows minimal drift in its surface climate. The atmospheric component of HadCM3 has 19 levels and a latitude/longitude resolution of 2.5x3.75 degrees, with grid of 96x73 points covering the globe. The resolution is about 417x278 km at the equator. The physical parameterization package of the model is very sophisticated. The radiative effects of minor greenhouse gases as well as CO_2, water vapour and ozone are explicitly represented. A parameterization of background aerosol is included. The land surface scheme includes freezing and melting of soil moisture, surface runoff and soil drainage. The convective scheme includes explicit down-draughts. Orographic and gravity wave drag are modelled. Cloud water is an explicit variable in the large-scale precipitation and cloud scheme. The atmospheric component of the model allows the emission, transport, oxidation and deposition of sulphur compounds to be simulated interactively. The oceanic component of HadCM3 has 20 levels with a horizontal resolution of 1.25x1.25 degrees, permitting important details in the oceanic current structure to be represented. The model is initialised directly from the observed ocean state at rest, with a suitable atmospheric and sea ice state. HadCM3 is being used for a wide range of climate studies which will form crucial inputs to the forthcoming Fifth Assessment Report (AR5) of the Intergovernmental Panel on Climate Change (IPPC), which will be finalized in 2014.

2.3 Downscaling and regional climate models

Global general circulation models are run at coarse spatial resolution, typically using a 100 km grid. They are unable to resolve many important sub-grid scale features such as clouds and topography. As a result, GCMs are not suitable for regional impact studies. To address this problem, various downscaling methods are employed to study local-scale climate impacts. The outputs of the global models are used as inputs to the regional models. The values generated during the execution of the global model are saved, and are used to specify the values around the boundaries of the limited domain, that is, the lateral boundary conditions. Wilby and Wigley (1997) identified four categories of downscaling: regression methods, weather pattern-based approaches, stochastic weather generators and limited-area modelling.

In the regression method, the fine details of the past climate are related to the coarse representation provided by the global model. Assuming the relationship holds under a different climate regime the regional details of the future climate can be deduced from coarse-grain predictions generated by the global model. This statistical downscaling has been used with some success. However, the hypothesis that the relationship between coarse and fine-grain structures remains unchanged under a changing climate is open to serious question. We therefore seek alternative approaches.

A regional Climate Model (RCM) uses the same physical principles and

mathematical equations as global models, but covers only a limited geographical domain. This allows us to use a much finer computational grid. Whereas a global model might have points separated by 100 km, a regional model would typically have a 10 km grid. Thus, it is capable of resolving a large range of atmospheric phenomena that 'fall between the gaps' of a GCM. In particular, the representation of mountains is much better in the RCM. Since temperature and precipitation are so strongly coupled with elevation and slope, this is a major advantage.

The climate scientists at UCD and at Met Éireann have been collaborating for several years on a project called the Community Climate Change Consortium for Ireland (C4I). The objective is to develop regional climate models and apply them to the question of Ireland's future climate. The main results to date are summarized in the report "Ireland in a Warmer World" (McGrath et al., 2008). The work has employed a range of regional models.

2.4 Uncertainty of the predictions

Climate models are the best means we have for predicting future changes in our climate. They have a solid scientific basis in the principles of physics, and they are increasing rapidly in sophistication and in the accuracy with which they can simulate the climate. However, the atmosphere is chaotic, that is, highly sensitive to very small changes, so that if the starting conditions are changed in a small way, the subsequent evolution will be completely different. Thus, no matter how good the models are, there will always be a degree of uncertainty in the predictions. There are many sources of uncertainty. Firstly, the initial state of the system is not known precisely. This is particularly the case for the deep ocean. Secondly, the external forcings cannot be known exactly; for example, the level of CO_2 twenty or forty years hence depends on population growth, and on energy use which may be strongly influenced by technological developments. The projections of future emissions of green-house gases strongly influence the predictions. Then the models themselves have imperfections, and many approximations must be made in constructing practical models. Next, the physical processes in the atmosphere and ocean are not completely understood, and are complex. Finally, there are many feedbacks in the climate system that make it very sensitive to small changes.

Among the processes that can act as positive feedbacks, we may consider the level of water vapour, the ice-albedo effect, cloud amount, carbon uptake by forest, and emission of methane from melting tundra. An increase of cloudiness may have either a cooling or a warming effect on climate, depending on the cloud height and structure. In general, low clouds act to cool the climate and high clouds have a warming effect. But in reality, things are much more complicated. For climate predictions over the next century, cloud feedbacks remain the greatest source of uncertainty (e.g. Soden and Held, 2006).

2.5 Probabilistic prediction: The ensemble approach

In view of the many uncertainties in predicting future climate, scientists now approach the problem from a stochastic point of view. For example, instead of trying to predict the increase of temperature by 2100 in a deterministic manner, we aim to predict both the most probable change and also the probable range of changes that may be observed. In essence, we try to forecast the probability density function rather than just a single deterministic value. To do this, we need to assess the sensitivity of the predictions to various errors in the initial state, in the model itself and in the specified external forcings. Considering a range of values of initial conditions and other parameters, we perform a collection of numerical predictions, called an ensemble. Depending on the available computer power, the ensemble may contain anything from a few predictions to as many as one hundred.

Using the ensemble outputs, we can examine how the predictions differ, and the extent to which they spread out from each other. If they form a compact set of closely-related values, we can be confident that the average of these values is a reliable guide to what may happen. If, however, they are widely dispersed, we may have relatively little confidence in the prediction. The IPCC predictions are generally based on ensembles of model runs, and are given in a probabilistic form. For example, the mean temperature increase under the assumptions of a particular emission scenario (A1B), is given as a "best estimate" of 2.8 K and a "likely range" between 1.7 K and 4.4 K.

3 Long-term climate change

3.1 Greenhouse and icehouse climates

A useful classification of Earth's climate types is into "icehouse climates", which feature large-scale continental ice sheets and widespread perennial sea ice at high latitudes, and "greenhouse climates", which do not. We are currently in an ice-house world, but Earth has switched between the two states several times during its history. Based mostly on the presence or absence of geological evidence for large-scale glaciation, Frakes et al. (1992) identify 5 icehouse periods separated by 4 greenhouse periods during the past 600 million years, each interval lasting 50–100 million years. Not all the cool periods identified are of the same intensity, though: as indicated in Figure 3, there is abundant evidence for two full-blown glaciations, during the early Carboniferous to mid Permian, 340–250 Ma, and the late Cenozoic (34 Ma to present), while the late Jurassic–early Cretaceous (183–105 Ma) and late Ordovician–early Silurian (458–421 Ma) cool periods may have seen only ephemeral ice sheets and seasonal sea ice.

Understanding how Earth shifts between greenhouse and icehouse is a central question in paleoclimatology. Changing levels of atmospheric greenhouse gas concentrations, especially CO_2, appear to play an important role in these

transitions. CO_2 reconstructions over the Phanerozoic are subject to much uncertainty, but they generally show reduced CO_2 levels during the Carboniferous–Permian and the late Cenozoic, qualitatively matching the glaciation record (Royer et al., 2004; Royer, 2006). There is also considerable modelling evidence that continental glaciation is controlled by CO_2 levels (see Section 3.4 below). The association between climate conditions and CO_2 is somewhat problematic for the end-Ordovician glaciation (440 Ma, see Figure 3), which occurred during a period of apparently high CO_2. The discrepancy may be due to the short duration of this glacial interval, which is possibly not well resolved by the CO_2 data. It should also be recalled that that insolation was around 3–4% lower than today at that time.

The question of what ultimately caused the CO_2 fluctuations over geological time is less settled. Long-term atmospheric CO_2 levels are controlled by the balance between the rate of volcanic outgassing and the rate of drawdown due to chemical weathering of silicate rocks (Walker et al., 1981; Berner et al., 1983). Plate tectonics can affect both source and sink: increased seafloor spreading rates or the subduction of carbonate-rich sediments will lead to increased outgassing, while the breakup of a supercontinent, continental drift from a temperate to a tropical zone and mountain uplift will all increase weathering rates and lead to reduced CO_2 levels. As a specific example, Kent and Muttoni (2008) suggest that high CO_2 during the early Cenozoic was due to the closing of Tethys (see Chapter X, this volume), a relatively shallow tropical ocean with deep carpet of carbonate sediments, whose subduction led to a period of increased outgassing. This period ended with the collision of India and Asia, which also brought the highly-weatherable Deccan Traps into the equatorial humid belt, explaining the subsequent decline in CO_2 through the Eocene and Oligocene. The evolution of land plants over geological time also had a major impact on the long-term carbon cycle, notably though the effect of root systems on weathering rates (Berner, 2004) and potentially through a host of other feedback loops (Beerling and Berner, 2005).

An important related question concerns the role of climate change in driving mass extinction events, particularly the 'big five' extinction events at the end-Ordovician (446 Ma), late Devonian (371 Ma), Permian-Triassic (PT) boundary (251 Ma), Triassic-Jurassic (TJ) boundary (200 Ma) and Cretaceous-Tertiary (KT) boundary (65 Ma) (Sepkoski, 1982). The PT, TJ and KT extinctions coincided with intense volcanism events, forming the Siberian Traps, Central Atlantic Magmatic Province and the Deccan Traps respectively, and the PT and TJ were also periods of rapidly rising CO_2 and temperature (McElwain et al., 1999; Benton and Twitchett, 2003). It is not clear however whether global warming by itself is sufficient to explain the mass extinctions (Mayhew et al., 2008), or whether other "kill mechanisms" need to be invoked. It is widely accepted that the KT extinction was associated with a large bolide impact (Alvarez et al., 1980), but there is scant evidence for such impacts during the other extinctions. Global warming can lead to sluggish oceanic circulation and widespread anoxia, which could explain extinction in the oceanic

realm (Kiehl and Shields, 2005). It has also been hypothesised that the emission of SO_2 and other pollutants from flood basalts may have had a directly noxious effect on biota, especially plants (van de Schootbrugge et al., 2009).

3.2 Neoproterozoic snowball Earth

In the most extreme case, the Earth can exist in a stable equilibrium where the oceans are entirely covered in ice. Whether this "snowball Earth" scenario has ever actually occurred remains contentious. A brief paper by Kirschvink (1992), noting evidence for low-latitude glaciation during the Neoproterozoic (~750 Ma), suggested a snowball Earth could have existed at that time. The idea was powerfully promoted by Hoffman et al. (1998), who provided more extensive evidence as well as a coherent narrative of how Earth could enter and exit such a state. The paper triggered a spurt of publications on the topic. While there is general consensus that the Neoproterozoic was an extreme icehouse period featuring low-latitude glaciation, the community is divided as to whether the planet was truly covered in ice, or rather the sea-ice line reached only to the subtropics, leaving a broad swath of open ocean in the tropics (the so-called "slushball Earth"). The two hypotheses are qualitatively different as regards their impacts on life: a true snowball would have killed off most marine life, since no light would have reached the underlying ocean through the thick layer of ice, while in a slushball scenario life could have continued relatively unperturbed in the tropics.

Climate model simulations suggest that a transition to a snowball Earth can indeed occur under Neoproterozoic conditions, though this is somewhat sensitive to the precise level of atmospheric CO_2 (e.g. Donnadieu et al., 2004). A greater difficulty with the snowball hypothesis concerns the exit mechanism. The basic idea (Caldeira and Kasting, 1992; Hoffman et al., 1998) is that, since the hydrological cycle comes to a halt during a snowball episode and the oceans are isolated from the atmosphere, there are no sinks for atmospheric CO_2, so given enough time sub-aerial volcanism will gradually build up large atmospheric CO_2 concentrations. Eventually, a threshold is crossed where tropical temperatures are high enough to melt the ice, at which point a catastrophic meltback ensues as the surface albedo feedback works in reverse. However, attempts to reproduce this process using a detailed climate model (Pierrehumbert, 2004, 2005) show that the system remains far short of deglaciation even at extremely elevated CO_2, on the order of 20% the total mass of the atmosphere. Thus, either the Earth was never in a snowball state, or other as yet unknown mechanisms explain the transition out of that state.

3.3 The early Cenozoic greenhouse

3.3.1 The early Eocene climate optimum

The early Cenozoic was a time of extreme global warmth, culminating in the early

Eocene "climate optimum" (EECO) around 50 Ma. Oxygen isotope proxies indicate benthic temperatures (which reflect high-latitude, annual-mean ocean surface conditions) could have been as high as 12°C (Zachos et al., 2001). Direct reconstruction of Arctic ocean surface temperatures using the TEX_{86} proxy suggest values as high as 19 °C (Sluijs et al., 2006). High-latitude continental interiors were also much warmer than today (Greenwood and Wing, 1995). In the tropics, recent sea surface temperature reconstructions using $\delta^{18}O$ in well-preserved foraminifera indicate temperatures in excess of 30 °C, independently confirmed by TEX_{86} estimates (Pearson et al., 2007). Overall, these reconstructions suggest a global-mean temperature during the EECO of perhaps 25 °C, around 10 °C higher than today.

Simulating the EECO poses a major challenge to climate models. Atmospheric CO_2 concentration during the EECO is known to have been much higher than today, with estimates ranging from around 1000 to 4000 ppm (compared to 280 ppm in modern pre-industrial times). Setting model CO_2 to values within this range, it is possible to match the 10 °C increase in global-mean temperature (Shellito et al., 2003), but it has proved impossible to capture the very weak equator-pole temperature gradient indicated by the proxy reconstructions. This "low-gradient paradox" suggests that current climate models may be missing some key physical ingredient responsible for the reduction in meridional temperature gradient.

Two types of explanation are possible: either some unknown or poorly represented radiative feedback acts to limit temperatures in the tropics or boost them at the poles, or dynamical atmosphere/ocean poleward heat transport increases much more rapidly with temperature than predicted by the models. Clouds, a known weakness of current climate models, play a major role in most explanations of the first type, either cooling the tropics (Lindzen et al., 2001) or warming the high latitudes (Sloan and Pollard, 1998; Abbot and Tziperman, 2008). As for the second category, it appears that poleward atmospheric heat transport in models cannot increase above a certain limit, for dynamical reasons that remain unclear (Caballero and Langen, 2005; O'Gorman and Schneider, 2008). Model ocean transports also do not increase much in coupled Eocene simulations (Huber and Sloan, 2001). Recent work has focused on the role of tropical cyclones, which are unresolved in current climate models and are therefore an ideal candidate for a "missing process". Tropical cyclone frequency and intensity are predicted to increase in a warmer world; by increasing vertical mixing in the ocean, this could lead to stronger poleward heat transport (Emanuel, 2001, 2002). However, direct implementation of a temperature-dependent ocean mixing rate in a climate model, designed to mimic the effect of tropical cyclones, failed to show much increase in heat transport to the high latitudes (Korty et al., 2008).

More recently, it has become apparent that much of the model-data discrepancy may actually be due to deficiencies in the data. While older temperature

reconstructions from pelagic foraminifera (e.g. Zachos et al., 1994) showed Eocene tropical temperatures comparable to or even lower than today, more recent studies using exceptionally well-preserved forams indicate much higher temperatures (Pearson et al., 2007), suggesting the colder estimates are biased low due to diagenesis. With these new tropical temperature estimates, the low-gradient paradox becomes much less severe.

3.3.2 Hyperthermals

The early Eocene is also exceptional in that it was punctuated by a series of "hyperthermals", short-lived events of extreme global warmth. Several such events have been documented recently (Lourens et al., 2005). The best-known hyperthermal, the Paleocene-Eocene Thermal Maximum (PETM), saw global temperature soar by over 5 ^{o}C in less than 10,000 years (Zachos et al., 2001), and then revert to pre-event levels over a longer period of about 150,000 years. The warming was accompanied by a sharp negative carbon isotope excursion (a reduction of the $^{12}C/^{13}C$ ratio) of global extent, and rapid shoaling of the calcite compensation depth indicative of ocean acidification (Zachos et al., 2005). The generally accepted interpretation of these facts is that a rapid injection of isotopically light carbon into the atmosphere caused a large, transient increase in the greenhouse effect, producing the rapid warming. The carbon anomaly was subsequently re-absorbed on the typical timescale associated with silicate rock weathering and oceanic deposition.

The origin of the requisite large, rapid carbon injection remains enigmatic. Several hypotheses have been put forward. The carbon could have been "baked" out of deep rocks by volcanic intrusions (Svensen et al., 2004), though this is hard to reconcile with the short-lived and recurrent nature of the events (Lourens et al., 2005). Catastrophic methane release from clathrate deposits has also been invoked (Dickens, 2003), though building large deposits under warm early Eocene conditions is difficult (Buffett and Archer, 2004). Finally, the isotopically light carbon could have come from the large-scale respiration of organic matter, possibly through the dessication of epicontinental seas (Higgins and Schrag, 2006).

Whatever its origin, the rapid carbon injection during hyperthermals is the closest known analog to the ongoing anthropogenic carbon release. In this context, hyperthermals provide a perspective on the kind of climate changes we may expect in future, as well as a unique opportunity to test the climate models used to predict these changes. The most recent estimate (Zeebe et al. 2009) puts the total carbon release during the PETM at no more than 3000 GtC, which would have resulted is somewhat less than a doubling of the pre-existing atmospheric CO_2 concentration. This is insufficient to explain the estimated global warming of 5 ^{o}C during the PETM, given the typical sensitivity of current climate models of around 3 ^{o}C per doubling of CO_2. Thus, if we believe these estimates to be correct, either some unknown positive feedbacks acted during the PETM to amplify the warming,

or the sensitivity of current climate models is biased towards low values.

3.4 Late Cenozoic glaciation

3.4.1 Glaciating Antarctica

Through the late Cretaceous and early Paleogene, the Earth was in a greenhouse state free of permanent continental ice sheets. Then, at the Eocene-Oligocene (EO) boundary (~34 Ma), a large ice sheet abruptly formed covering Antarctica. The transition is marked by a step-like rise in the benthic $\delta^{18}O$ record (see Figure 2). Early work (Kennett, 1977) conjectured that the transition was tectonically driven, coinciding with the separation of Australia from Antarctica. The opening of the Tasman Gateway created a continuous ocean belt around Antarctica, bringing the Antarctic Circumpolar Current into existence and supposedly interrupting the southward flow of warm water from the subtropics which existed previously. The resulting "thermal isolation" of Antarctica would then have led to its glaciation. A study using a simplified ocean-atmosphere model (Sijp and England, 2004) showed that opening a circumpolar seaway would indeed give a modest cooling over Antarctica. On the other hand, simulations using a full-physics coupled ocean-atmosphere climate model under late Eocene conditions (Huber et al., 2004) showed that Antarctica was in fact "thermally isolated" even before the opening of the Tasman Gateway: no warm subtropical currents reached high southern latitudes even with Tasmania attached to Antarctica.

An entirely different scenario for the onset of Antarctic glaciation was proposed by DeConto and Pollard (2003). They ran a global atmospheric model with late Eocene topography coupled to an ice sheet model, and gradually reduced the level of atmospheric CO_2. They found that once the concentration dropped below a threshold level, an ice sheet abruptly and spontaneously appeared over Antarctica. Though the change in CO_2 was gradual, the build-up of the ice sheet was rapid due to the strong feedbacks at play. The most obvious such feedback involves surface albedo: ice and snow are much more reflective than most other types of surface cover, so their presence reduces net absorbed insolation and leads to lower temperatures, promoting further ice formation. Additionally, increasing ice sheet height enhances mass gain during winter and reduces mass loss during summer (because a high ice sheet top is colder and therefore less subject to melting), so that the ice sheet's mass balance becomes increasingly positive the larger it grows; this positive feedback is finally halted by downhill ice flow once the ice sheet becomes sufficiently massive. Antarctica, having high orography near the pole, is particularly sensitive to this mechanism, while the Arctic, with an ocean around the pole and no high orography on the surrounding continents, requires much lower levels of CO_2 to form an ice sheet.

3.4.2 Glaciating the Arctic

While the early Oligocene emplacement of a continental-scale Antarctic ice sheet is

well established, the time of first appearance of ice sheets in the Northern Hemisphere remains controversial. Recent work shows evidence for ice-rafted debris in the Northern Hemisphere during the Eocene and early Oligocene (Eldrett et al., 2007; Tripati et al., 2008). Moreover, paleothermometry studies using Mg/Ca isotopes suggest little benthic temperature change across the EO boundary, implying that the entire 1.5 ‰ shift in $\delta^{18}O$ is attributable to ice-sheet growth (Billups and Schrag, 2003; Coxall et al., 2005). A shift this large would require more ice growth than can be accommodated on Antarctica. Overall, this new evidence suggests that Northern Hemisphere ice sheets appeared in the early Oligocene, and the EO boundary glaciation was in fact bipolar. However, DeConto et al. (2008) find that Arctic glaciation requires CO_2 concentration to drop below 280 ppm in their atmosphere-ice sheet coupled model, a level far below that which prevailed during the early Oligocene according to the paleo-CO_2 reconstruction of Pagani et al. (2005). In addition, paleotemperature reconstruction using the TEX_{86} proxy (Liu et al., 2009) shows that high-latitude sea surface temperatures dropped by about 5°C across the EO boundary. This cooling can account for much of the oxygen observed isotopic excursion, and the remaining fraction can be explained by an ice volume that can be comfortably accommodated on Antarctica alone. The evidence for ice-rafted debris can be explained by localised, ephemeral ice caps on the higher orography.

The final transition to the modern icehouse world, including orbitally-paced waxing and waning of continental-scale Northern Hemisphere ice sheets, is thought to have occurred in the late Pliocene, ~2.7 Ma (Shackleton et al., 1984). Several mechanisms have been proposed for this transition, and there is as yet no clear consensus on which was the dominant one. The "Panamanian hypothesis" (Keigwin, 1982) notes the rough coincidence between glacial onset and final closure of the Panamanian seaway. By preventing mixing of Atlantic and Pacific waters, this closure could have increased the strength of the Atlantic "conveyor belt" circulation, increasing the supply of moisture to the Greenland and ultimately feeding a larger ice sheet. Atlantic temperature proxy data provide some support for this scenario (Bartoli et al., 2005). The "uplift hypothesis" suggests that the rise of the Rockies and Himalayan Plateau during the Cenozoic would have altered atmospheric circulation patterns, making Greenland's climate cooler, moister and more conducive to ice sheet formation (Ruddiman and Kutzbach, 1989). A more recent hypothesis points to evidence that during the late Miocene and early Pliocene, the tropical Pacific was in a "permanent El Niño" state, i.e. one with permanently warm conditions in the eastern basin and no east-west equatorial temperature gradient (Wara et al., 2005). Transition to the modern regime, with cooler average conditions in the east and interannual fluctuations between El Niño (warm) and La Niña (cool) events, roughly coincides with glacial onset. Noting the modern observed impacts of El Niño events on high-latitude climate, some authors have drawn a causal connection between the two transitions (Molnar and Cane, 2002; Philander and Fedorov, 2003). Finally, it is possible that CO_2 concentrations

decreased through the Pliocene (Lunt et al., 2008), bringing the system across the threshold for Arctic glaciation (DeConto et al., 2008). A test of all these hypotheses using a comprehensive atmosphere-ocean-ice sheet model (Lunt et al., 2008) found that only a drop in CO_2 could fully account for glacial onset. Furthermore, model-date comparison by Huber and Caballero (2003) showed that an active ENSO cycle probably existed during the Eocene, when all conditions for a "permanent El Niño" were satisfied, so it is difficult to see what could have induced such a state in the Miocene.

4 Summary

Earth's climate system fluctuates on all timescales, from hours to billions of years. Over its history, Earth has gone through a succession of greenhouse and icehouse states, which correlate well with periods of high and low atmospheric CO_2 concentration. Climate modelling is playing an increasingly important role in unravelling the intricate details of these transitions. At the same time, paleoclimate applications expose some of the greatest limitations of current models. In particular, paleoclimate proxy data from the very warm climates of the early Eocene suggest climate models may substantially underestimate the sensitivity of surface temperature to CO_2, particularly at high latitudes. While the long-standing "low-gradient paradox" may be nearing resolution due to improved paleotemperature estimates (see Section 3.3.1), the emerging challenge is to explain how paleoclimates may have become so warm with relatively modest levels of CO_2. Changes in clouds, perhaps linked to changes in ocean biota (Kump and Pollard, 2008), may provide part of the answer. This provides an exciting avenue for future research in bio-climate interactions.

References

Abbot, D. and E. Tziperman, 2008: Sea ice, high-latitude convection, and equable climates. *Geophys. Res. Lett.*, **35**, L03 702.

Alvarez, L., W. Alvarez, F. Asaro, and H. Michel, 1980: Extraterrestrial cause for the Cretaceous-Tertiary extinction. *Science*, **208**, 1095.

Bartoli, G., M. Sarnthein, M. Weinelt, H. Erlenkeuser, D. Garbe-Schönberg, and D. Lea, 2005: Final closure of Panama and the onset of northern hemisphere glaciation. *Earth Planet. Sci. Lett.*, **237**, 33–44.

Beerling, D. and R. Berner, 2005: Feedbacks and the coevolution of plants and atmospheric CO_2. *Proc. Natl. Acad. Sci. USA*, **102**, 1302–1305.

Benton, M. and R. Twitchett, 2003: How to kill (almost) all life: the end-Permian extinction event. *Trends Ecol. Evol.*, **18**, 358–365.

Beran, J., 1994: *Statistics for Long-Memory Processes*. Monographs on Statistics and Applied Probability, Chapman & Hall/CRC.

Berner, R., 2004: *The phanerozoic carbon cycle: CO_2 and O_2*. Oxford University Press, Oxford.

Berner, R., A. Lasaga, and R. Garrels, 1983: The carbonate-silicate geochemical cycle and its effect on atmospheric carbon dioxide over the past 100 million years. *Am. J. Sci*, **283**, 641–683.

Billups, K. and D. Schrag, 2003: Application of benthic foraminiferal Mg/Ca ratios to questions of Cenozoic climate change. *Earth Planet. Sci. Lett.*, **209**, 181–195.

Buffett, B. and D. Archer, 2004: Global inventory of methane clathrate: sensitivity to changes in the deep ocean. *Earth Planet. Sci. Lett.*, **227**, 185–199.

Charney, J. G., R. Fjørtoft and J. von Neumann, 1950: Numerical integration of the barotropic vorticity equation. *Tellus*, **2**, 237-254.

Caballero, R. and P. Langen, 2005: The dynamic range of poleward energy transport in an atmospheric general circulation model. *Geophys. Res. Lett.*, **32**, L02705, doi: 10.1029/2004GL021581.

Caldeira, K. and J. Kasting, 1992: Susceptibility of the early Earth to irreversible glaciation caused by carbon dioxide clouds. *Nature*, **359**, 226–228.

Coxall, H., P. Wilson, H. Pälike, C. Lear, and J. Backman, 2005: Rapid stepwise onset of Antarctic glaciation and deeper calcite compensation in the Pacific Ocean. *Nature*, **433**, 53–57.

DeConto, R. and D. Pollard, 2003: Rapid Cenozoic glaciation of Antarctica induced by declining atmospheric CO_2. *Nature*, **421**, 245–249.

DeConto, R., D. Pollard, P. Wilson, H. Pälike, C. Lear, and M. Pagani, 2008: Thresholds for Cenozoic bipolar glaciation. *Nature*, **455**, 652–656.

Dickens, G., 2003: Rethinking the global carbon cycle with a large, dynamic and microbially mediated gas hydrate capacitor. *Earth Planet. Sci. Lett.*, **213**, 169– 183.

Donnadieu, Y., Y. Godderis, G. Ramstein, A. Nedelec, and J. Meert, 2004: A snowball Earth climate triggered by continental break-up through changes in runoff. *Nature*, **428**, 303–306.

Eldrett, J., I. Harding, P. Wilson, E. Butler, and A. Roberts, 2007: Continental ice in Greenland during the Eocene and Oligocene. *Nature*, **446**, 176–179.

Emanuel, K., 2001: Contribution of tropical cyclones to meridional heat transport by the oceans. *J. Geophys. Res.*, **106**, 14 771–14 781.

Emanuel, K., 2002: A simple model for multiple climate regimes. *J. Geophys. Res.*, **107**, 10.1029/2001JD001 002.

Frakes, L., J. Francis, and J. Syktus, 1992: *Climate modes of the Phanerozoic*. Cambridge University Press Cambridge.

Greenwood, D. R. and S. L. Wing, 1995: Eocene continental climates and latitudinal temperature gradients. *Geology*, **23**, 1044–1048.

Higgins, J. and D. Schrag, 2006: Beyond methane: towards a theory for the Paleocene–Eocene thermal maximum. *Earth Planet. Sci. Lett.*, **245**, 523–537.

Hoffman, P. F., A. J. Kaufman, G. P. Halverson, and D. P. Schrag, 1998: A Neoproterozoic snowball Earth. *Science*, **281**, 1342–1346.

Huber, M., H. Brinkhuis, C. Stickley, K. Doos, A. Sluijs, J.Warnaar, S. Schellenberg, and G.Williams, 2004: Eocene circulation of the Southern Ocean: Was Antarctica kept warm by subtropical waters? *Paleoceanography*, **19**, PA4026.

Huber, M. and R. Caballero, 2003: Eocene El Niño: Evidence for robust tropical dynamics in the "hothouse". *Science*, **299**, 877–881.

Huber, M. and L. Sloan, 2001: Heat transport, deep waters and thermal gradients: Coupled climate simulation of an Eocene greenhouse climate. *Geophys. Res. Lett.*, **28**, 3841–3884.

Huybers, P. and W. Curry, 2006: Links between annual, Milankovitch and continuum temperature variability. *Nature*, **441**, 329–332.

Keigwin, L., 1982: Isotopic paleoceanography of the Caribbean and East Pacific: role of Panama uplift in late Neogene time. *Science*, **217**, 350.

Kennett, J., 1977: Cenozoic evolution of Antarctic glaciation, the circum-Antarctic Ocean, and their impact on global paleoceanography. *J. Geophys. Res.*, **82**, 3843–3860.

Kent, D. and G. Muttoni, 2008: Equatorial convergence of India and early Cenozoic climate trends. *Proc. Natl. Acad. Sci. USA*, **105**, 16 065.

Kiehl, J. and C. Shields, 2005: Climate simulation of the latest Permian: Implications for mass extinction. *Geology*, **33**, 757–760.

Kirschvink, J., 1992: Late Proterozoic low-latitude global glaciation: the snowball Earth. *The Proterozoic Biosphere*, 51–52.

Korty, R., K. Emanuel, and J. Scott, 2008: Tropical cyclone–induced upper-ocean mixing and climate: Application to equable climates. *J. Climate*, **21**, 638–654.

Kump, L. and D. Pollard, 2008: Amplification of Cretaceous warmth by biological cloud feedbacks. *Science*, **320**, 195.

Kutzbach, J. E., 1976: The nature of climate and climatic variations. *Quaternary Res.*, **6**, 471–480.

Lewis, J. M., 1998: Clarifying the dynamics of the general circulation: Phillips's 1956 experiment. *Bull. Amer. Meteor. Soc*., **79**, 39-60

Lindzen, R., M. Chou, and A. Hou, 2001: Does the earth have an adaptive infrared iris? *Bull. Amer. Meteor. Soc.*, **82**, 417–432.

Liu, Z., et al., 2009: Global cooling during the Eocene-Oligocene climate transition. *Science*, **323**, 1187–1190.

Lourens, L., A. Sluijs, D. Kroon, J. Zachos, E. Thomas, U. Röhl, J. Bowles, and I. Raffi, 2005: Astronomical pacing of late Palaeocene to early Eocene global warming events. *Nature*, **435**, 1083–1087.

Lunt, D., G. Foster, A. Haywood, and E. Stone, 2008: Late Pliocene Greenland glaciation controlled by a decline in atmospheric CO_2 levels. *Nature*, **454**, 1102–1105.

Lynch, P., 2006: *The emergence of numerical weather prediction: Richardson's dream*. Cambridge Univ Press, 279pp.

Mayhew, P., G. Jenkins, and T. Benton, 2008: A long-term association between global temperature and biodiversity, origination and extinction in the fossil record. *Proc. R. Soc. B*, **275**, 47–53.

O'Gorman, P. and T. Schneider, 2008: The hydrological cycle over a wide range of climates simulated with an idealized GCM. *J. Climate*, **21**, 3815–3832.

McElwain, J., D. Beerling, and F. Woodward, 1999: Fossil plants and global warming

at the Triassic-Jurassic boundary. *Science*, **285**, 1386.

McGrath, R., et al., 2008: Ireland in a warmer world: Scientific predictions of the Irish climate in the twenty-first century. Tech. rep., Met Éireann.

Mitchell, J., 1976: An overview of climatic variability and its causal mechanisms. *Quaternary Res*, **6**, 481–493.

Molnar, P. and M. A. Cane, 2002: El Niño's tropical climate and teleconnections as a blueprint for pre-Ice Age climates. *Paleoceanography*, **17**, 11.

Pagani, M., J. Zachos, K. Freeman, B. Tipple, and S. Bohaty, 2005: Marked decline in atmospheric carbon dioxide concentrations during the Paleogene. *Science*, **309**, 600–603.

Pearson, P., B. Van Dongen, C. Nicholas, R. Pancost, S. Schouten, J. Singano, and B. Wade, 2007: Stable warm tropical climate through the Eocene Epoch. *Geology*, **35**, 211.

Philander, S. G. and A. V. Fedorov, 2003: Role of tropics in changing the response to Milankovich forcing some three million years ago. *Paleoceanography*, **18**, 1045.

Phillips, N., 1956: The general circulation of the atmosphere: A numerical experiment. *Quart. J. Roy. Meteor. Soc.*, **82**, 123–164.

Pierrehumbert, R. T., 2004: High levels of atmospheric carbon dioxide necessary for the termination of global glaciation. *Nature*, **429**, 646–649.

Pierrehumbert, R. T., 2005: Climate dynamics of a hard snowball Earth. *J. Geophys. Res.*, **110**, D1111, doi: 10.1029/2004JD005 162. 26

Royer, D., 2006: CO_2-forced climate thresholds during the Phanerozoic. *Geochim. Cosmochim. Acta*, **70**, 5665–5675.

Royer, D., R. Berner, I. Montañez, N. Tabor, and D. Beerling, 2004: CO_2 as a primary driver of Phanerozoic climate. *GSA Today*, **14**, 5.

Ruddiman, W. and J. Kutzbach, 1989: Forcing of late Cenozoic Northern Hemisphere climate by plateau uplift in southern Asia and the American West. *J. Geophys. Res.*, **94**, 18 409–18 427.

Sagan, C. and G. Mullen, 1972: Earth and Mars: evolution of atmospheres and surface temperatures. *Science*, **177**, 52–56.

Sepkoski, J. J., 1982: Mass extinctions in the Phanerozoic oceans: a review. *Geol. Soc. Am. Spec. Pap.*, **191**, 283–289.

Shackleton, N., et al., 1984: Oxygen isotope calibration of the onset of ice-rafting and history of glaciation in the North Atlantic region. *Nature*, **307**, 620–623.

Shaviv, N. and J. Veizer, 2003: Celestial driver of Phanerozoic climate? *GSA Today*, **13**, 4–10.

Shellito, C. J., L. C. Sloan, and M. Huber, 2003: Climate sensititvity to atmospheric CO_2 levels in the Early–Middle Paleogene. *Paleogeogr. Paleoclimatol. Paleoecol.*, **193**, 113–123, doi:10.1016/S0031-0182(02)00718-6.

Sijp, W. and M. England, 2004: Effect of the Drake Passage throughflow on global climate. *J. Phys. Oceanogr.*, **34**, 1254–1266.

Sloan, L. C. and D. Pollard, 1998: Polar stratospheric clouds: A high latitude warming mechanism in an ancient greenhouse world. *Geophys. Res. Lett.*, **25**, 3517–3520.

Sluijs, A., et al., 2006: Subtropical Arctic Ocean temperatures during the Palaeocene/Eocene thermal maximum. *Nature*, **441**, 610–613.

Soden, B. and I. Held, 2006: An assessment of climate feedbacks in coupled ocean–atmosphere models. *J. Climate*, **19**, 3354–3360.

Solomon, S., D. Qin, M. Manning, M. Marquis, K. Averyt, M. Tignor, H. Miller, and Z. Chen, 2007: *Climate change 2007: the physical science basis; Contribution of Working Group I to the fourth Assessment Report of the Intergovenmental Panel on Climate Change*. Cambridge Univ. Press.

Svensen, H., S. Planke, A. Malthe-S.renssen, B. Jamtveit, R. Myklebust, T. Eidem, and S. Rey, 2004: Release of methane from a volcanic basin as a mechanism for initial Eocene global warming. *Nature*, **429**, 542–545.

Tripati, A., et al., 2008: Evidence for glaciation in the Northern Hemisphere back to 44 Ma from ice-rafted debris in the Greenland Sea. *Earth Planet. Sci. Lett.*, **265**, 112–122.

van de Schootbrugge, B., et al., 2009: Floral changes across the Triassic/Jurassic boundary linked to flood basalt volcanism. *Nat. Geosci.*, **2**, 589–594.

Walker, J., P. Hays, and J. Kasting, 1981: A negative feedback mechanism for the long-term stabilization of the Earth's surface temperature. *J. Geophys. Res.*, **86**,

9776–9782.

Wara, M., A. Ravelo, and M. Delaney, 2005: Permanent El Ni˜no-like conditions during the Pliocene warm period. *Science*, **309**, 758–761.

Washington, W. and C. Parkinson, 2005: *An introduction to three-dimensional climate modeling*. University Science Books, 353 pp.

Wilby, R. and T. Wigley, 1997: Downscaling general circulation model output: a review of methods and limitations. *Prog. Phys. Geog.*, **21**, 530–548.

Wilson, J., 1966: Did the Atlantic Close and then Re-Open? *Nature*, **211**, 676–681.

Wunsch, C., 2003: The spectral description of climate change including the 100 ky energy. *Clim. Dyn.*, **20**, 353–363.

Wunsch, C., 2004: Quantitative estimate of the Milankovitch-forced contribution to observed Quaternary climate change. *Quat. Science Rev.*, **23**, 1001–1012.

Zachos, J., M. Pagani, L. Sloan, E. Thomas, and K. Billups, 2001: Trends, rythms and aberrations in global climate 65 Ma to present. *Science*, **292**, 686–693.

Zachos, J., L. Stott, and K. Lohmann, 1994: Evolution of early Cenozoic marine temperatures. *Paleoceanography*, **9**, 353–387.

Zachos, J., et al., 2005: Rapid acidification of the ocean during the Paleocene-Eocene thermal maximum. *Science*, **308**, 1611–1615.

Zeebe, R.E. and Zachos, J.C. and Dickens, G.R., 2009: Carbon dioxide forcing alone insufficient to explain Palaeocene-Eocene Thermal Maximum warming. *Nat. Geo.,* **2**, 576-580.

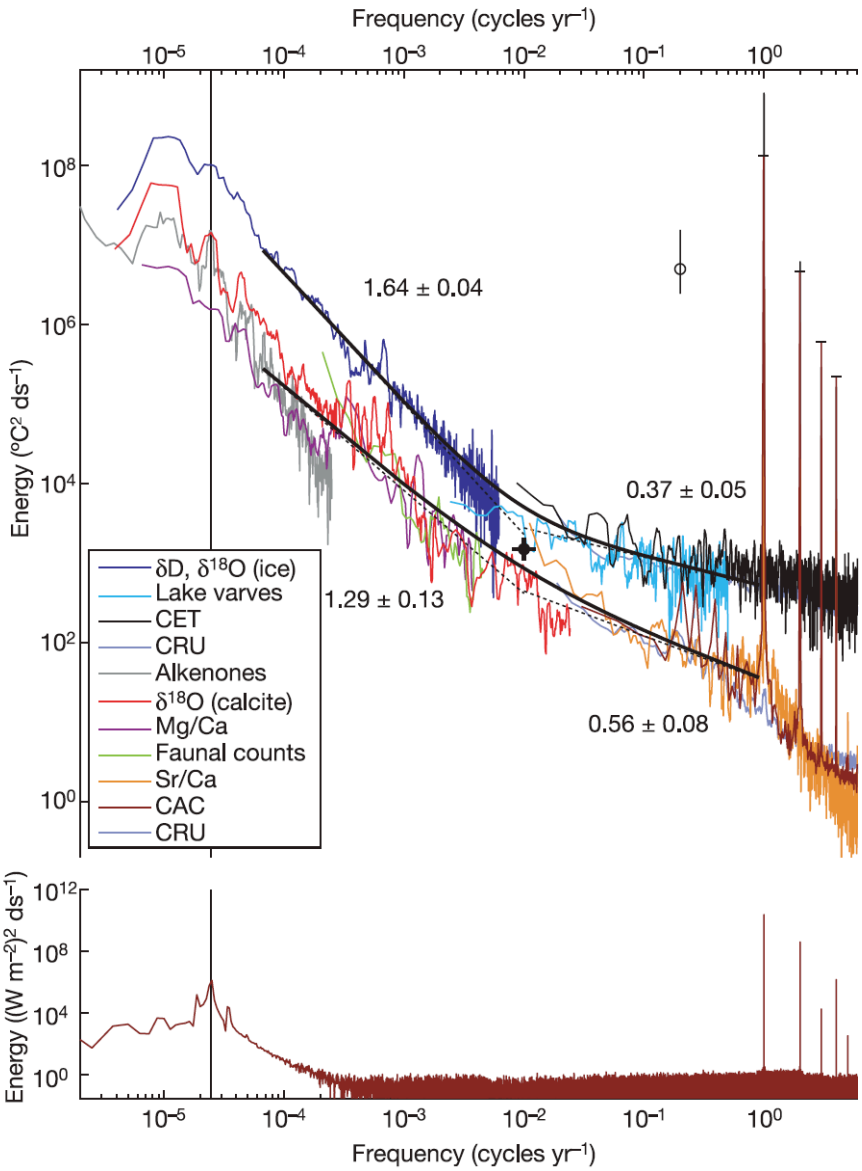

Figure 1: Patch-work spectral estimate using instrumental and proxy records of surface temperature variability. The more-energetic spectral estimate is from high-latitude continental records and the less-energetic estimate from tropical sea surface temperatures. Power-law estimates between 1.1–100 yr and 100–15,000 yr periods are listed along with standard errors, and indicated by the dashed lines. The sum of the power-laws fitted to the long- and short-period continuum are indicated by the black curve. The vertical line-segment indicates the approximate 95% confidence interval, where the circle indicates the background level. The mark at 1/100 yr indicates the region mid-way between the annual and Milankovitch periods. At bottom is the spectrum of insolation at 65N sampled monthly over the past million years plus a small amount of white noise. The vertical black line indicates the 41-kyr obliquity period. Taken from Huybers and Curry (2006).

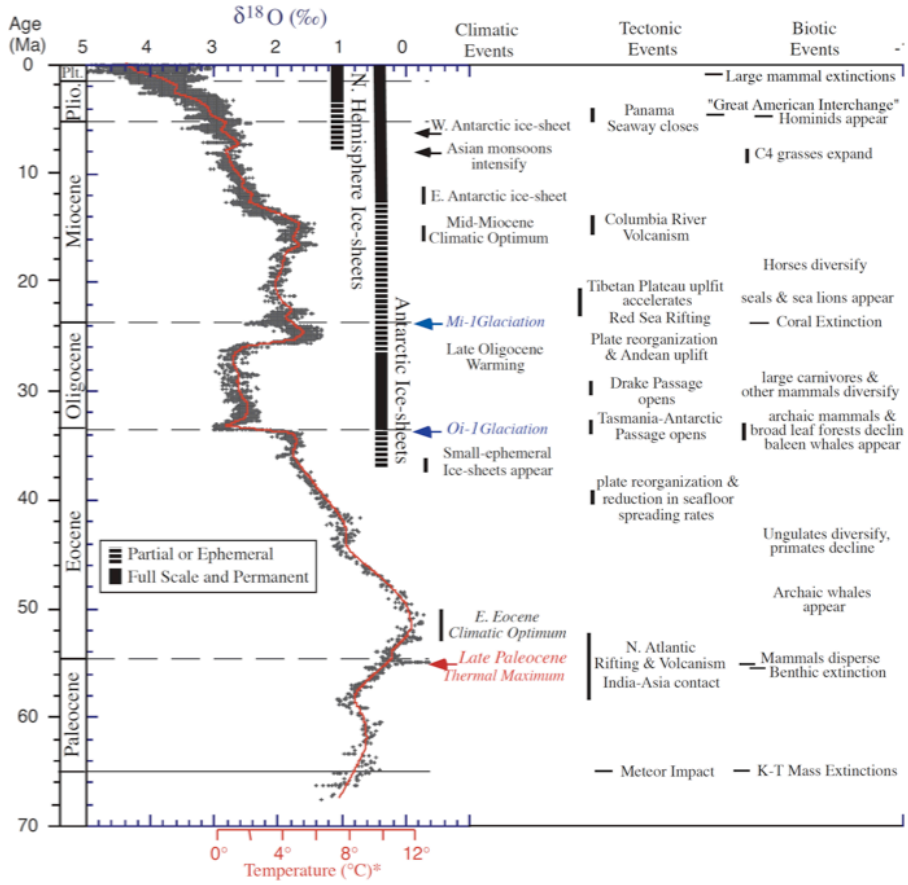

Figure 2: Global deep-sea oxygen isotope records for the Cenozoic era, based on data compiled from more than 40 ocean drilling sites. The raw data were smoothed using a five-point running mean, and curve-fitted with a locally weighted mean. The oxygen isotope temperature scale was computed for an ice-free ocean, and thus only applies to the time preceding the onset of large-scale glaciation on Antarctica (35 Ma). From the early Oligocene to present, much of the variability in the oxygen isotope record reflects changes in Antarctica and Northern Hemisphere ice volume. The vertical bars provide a rough qualitative representation of ice volume in each hemisphere relative to the Last Glacial Maximum (21 kyr ago), with the dashed bar representing periods of minimal ice coverage (less than 50%), and the full bar representing close to maximum ice coverage (more than 50% of present). Some key tectonic and biotic events are listed as well. Adapted from Zachos et al. (2001); see original paper for further details.

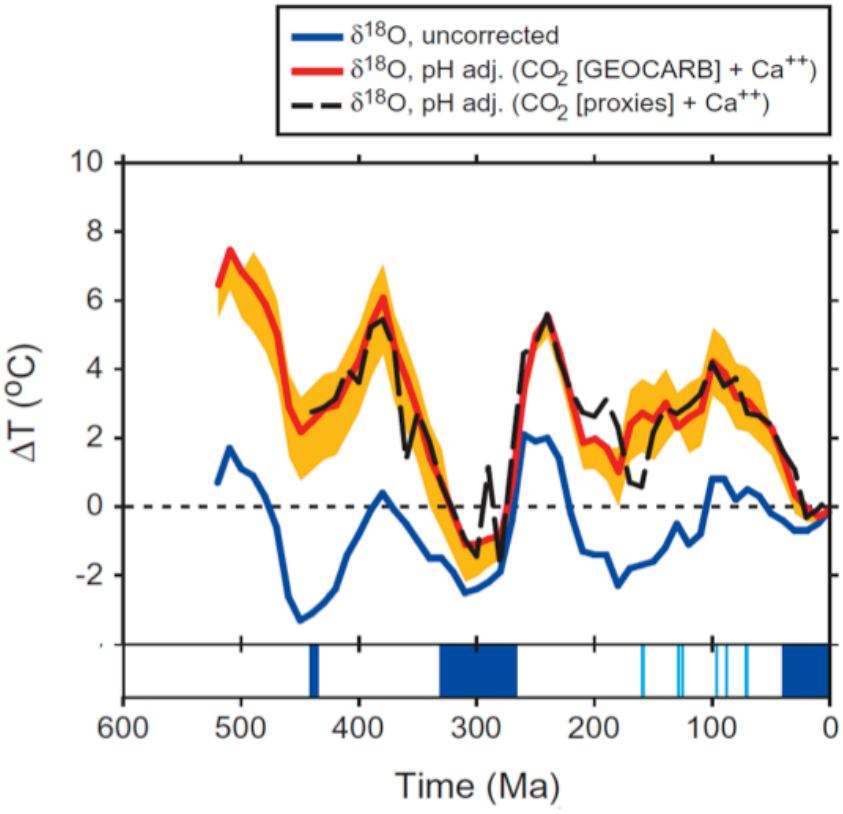

Figure 3: Shallow marine carbonate oxygen isotope record over the Phanerozoic aeon. The blue curve corresponds to temperature deviations relative to today calculated by (Shaviv and Veizer, 2003). In the two remaining curves, data from the blue curve have been adjusted for pH effects due to changes in seawater calcium ion concentration and CO_2 based either on model (GEOCARB) or proxy reconstructions. Blue bands in the strip along the bottom indicate "icehouse" intervals, with extensive, permanent continental ice sheets (dark blue) or cool climates, with modest, ephemeral ice sheets (light blue). Adapted from (Royer et al., 2004); see original paper for further details.